

# Fabrication of MgO nanoparticulates reinforced aluminum matrix composites using stir-casting method

H. Abdizadeh<sup>1,2</sup>, P. H. Vajargah<sup>1</sup>, M. A. Baghchesara<sup>3\*</sup>

<sup>1</sup>*School of Metallurgy & Materials Engineering, College of Engineering, University of Tehran, P.O. Box 14395-553, Tehran, Iran*

<sup>2</sup>*Center of Excellence for High Performance Materials, University of Tehran, P.O. Box 14395-553, Tehran, Iran*

<sup>3</sup>*Department of Metallurgy and Materials Engineering, Masjed Soleiman Branch, Islamic Azad University, Masjed Soleiman, Iran*

Received 27 June 2014, received in revised form 24 July 2014, accepted 19 December 2014

## Abstract

In the present work, A356.1 aluminum alloy matrix composites reinforced with 1.5, 2.5, and 5 vol.% MgO nanoparticles were fabricated at various casting temperatures, viz. 800, 850 and 950 °C using stir casting method. Density, crystal structure and microstructure of the samples were investigated in order to achieve the optimum amount of casting temperature. Also, the composites were characterized by scanning electron microscopy (SEM) and X-ray diffraction (XRD). Results indicated that with increasing the content of the second phase (MgO), the amount of agglomeration and porosity increased. However, the microstructural characterization of the composite samples showed uniform distribution of reinforcement and presence of the minimal porosity. Density results showed adjacent values in comparison with theoretical ones. Composite cast at 850 °C can be considered as the optimum fabrication conditions.

**Key words:** aluminum matrix composite, stir casting, MgO nanoparticles, microstructure, density

## 1. Introduction

Generally, composite materials are divided into three major categories, viz. metal matrix composites, polymer matrix composites and ceramic matrix composites. Metal matrix composites are considered as a group of advanced materials which represent improved properties [1, 2].

Metal matrix nanocomposites (MMNCs) attract great deals of attention nowadays due to their great mechanical properties and also their further applications in advanced industries [3–7].

The aim involved in designing metal matrix composite materials is to combine the desirable attributes of metals and ceramics. The addition of high strength, high modulus refractory particles to a ductile metal matrix produce a material whose mechanical properties are intermediate between the matrix alloy and the ceramic reinforcement. Metals have a useful combination of properties such as high strength, ductility and

high temperature resistance, but sometimes have low stiffness, whereas ceramics are stiff and strong, though brittle [8, 9].

Various kinds of methods have been used for fabrication of Al matrix nanocomposites like infiltration [10], squeeze casting [11], mechanical alloying [12], powder metallurgy [13, 14], ball milling [15], and stir casting [16]. Among the variety of manufacturing processes available for discontinuous metal matrix composites, stir casting technique for producing metal matrix composites (MMCs) has been developed to manufacture a wide range of engineering components due to its simplicity, flexibility and applicability to large quantity production. It is also attractive because, in principle, it allows a conventional metal processing route to be used, and hence minimizes the final cost of the product [9, 17].

Aluminum is one of the best materials for matrix because of its low density, corrosion resistance, high conductivity, and high toughness [18]. Different types

\*Corresponding author: tel.: (+98) 919 4798823; fax: (+98) 21 88 00 6076; e-mail addresses: [m.a.baghchehsara@iaumis.ac.ir](mailto:m.a.baghchehsara@iaumis.ac.ir), [amsara2000@gmail.com](mailto:amsara2000@gmail.com)

Table 1. Chemical composition of A356.1 Al alloy

Element	Al	Si	Fe	Cu	Mg	Mn	Zn	Ti	Ni
Mass%	91.73	7.23	0.32	0.18	0.38	0.02	0.05	0.01	0.05

of ceramic nanoparticles such as  $\text{Al}_2\text{O}_3$ ,  $\text{B}_4\text{C}$ , and  $\text{SiC}$  [19–21], have been implemented for Al matrix nanocomposites. MgO due to its high melting point ( $T_m = 2800^\circ\text{C}$ ), compressive strength, hardness, and also excellent thermodynamic stability is an appropriate choice for reinforcement [22, 23].

The behavior of particulates at the solid/liquid interface has attracted the interest of many researchers over the past several years [24–26]. This is because the mechanical properties of particulate composites are mainly controlled by the distribution of the particulates. Therefore, the most important characteristics is the interaction of particulates with the solid/liquid interface. The uniform distribution is required for the strengthening of the composites [27–30].

Therefore, formation of solidification microstructure in cast particulate composites is mainly influenced by nucleation, or its absence, on particulates and particulate pushing or engulfment by the solidification front. In spite of the extensive research done world-wide over the last quarter of the 20th century on cast MMCs, understanding of the phenomena occurring during solidification of these advanced materials is far from complete [27, 31–34].

In summary, in order to achieve the optimum properties of the metal matrix composite, the distribution of the reinforcement material in the matrix alloy must be uniform, and the wettability or bonding between these substances should be optimized. The porosity levels need to be minimized, and chemical reactions between the reinforcement materials and the matrix alloy must be avoided [8].

In the present study, Al-MgO nanocomposites were fabricated by the stir casting method with different volume percents of MgO content (as the reinforcement phase), and casting temperatures (totally, 9 distinct conditions). Subsequently, fabricated samples were used for the density test, and also SEM and XRD analysis.

## 2. Materials and methods

In this study, A356.1 aluminum alloy was used as the matrix material while MgO powder (with average diameter of 70 nm) was used as the reinforcement, and the composites were produced using a stir-casting method. The chemical composition of the Al alloy is shown in Table 1. The fabrication steps as well as their detail information, for stir casting method, were

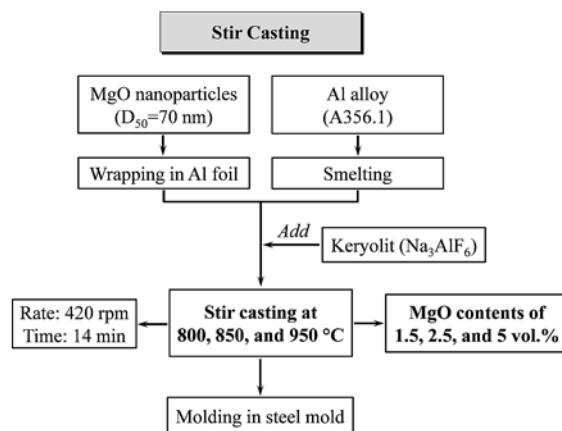


Fig. 1. Flowchart representation of stir casting method for fabrication of Al/MgO nanocomposite.

brought as flowchart diagram in Fig. 1. In order to manufacture the composites, the aluminum alloy was melted at 800, 850 and 950 °C, using a furnace and an impeller which was made of graphite. The melt was stirred at a constant speed of 420 rpm for 14 min and the different amount of MgO particles (1.5, 2.5, and 5 vol.%) were added (which were wrapped in Al foil) into the molten alloy. Stirring was carried out for 2 more minutes and the molten composites were poured inside a metallic mold (cylindrical shape with 15 cm height and 15 mm diameter).

To investigate the density of the fabricated specimens, a density test system was used to measure density according to the Archimedes method. After that, X-ray diffraction (XRD) method was performed for crystal structure and phase investigation via Philips PW1800 X-ray diffractometer ( $\text{CuK}\alpha$  radiation,  $\lambda = 1.5405 \text{ \AA}$ , 40 kV, 30 mA). Finally, Scanning Electron Microscopy (SEM) and X-ray mapping were implemented on polished (down to 1  $\mu\text{m}$ ) and etched (with Keller solution) samples to investigate morphological and microstructural aspects of the nanocomposites using Oxford CamScan MV2300, UK.

## 3. Results and discussion

### 3.1. Density measurements

Bulk density, theoretical density, and the porosity factor ( $\varepsilon$ ) for each MgO volume percent and cast-

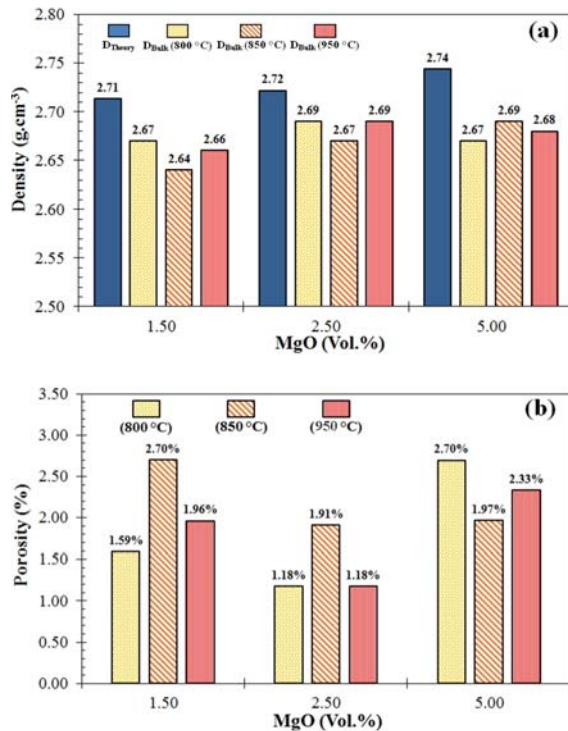


Fig. 2. Theoretical and bulk density of Al/MgO nanocomposites with different amounts of MgO reinforcement phase cast at different temperatures of 800, 850 and 950 °C (a), and porosity factors of the same samples (b).

ing temperature are presented in Fig. 2a,b. Theoretical density of the composites is calculated according to the rule of mixtures (Eq. (1)) assuming the densities of aluminum alloy and MgO equal to 2.70 and 3.58 g cm<sup>-3</sup>, respectively:

$$\rho_{\text{composite}} = \rho_{\text{Al}}\chi_{\text{Al}} + \rho_{\text{TiB}_2}\chi_{\text{TiB}_2}, \quad (1)$$

where  $\rho$  stands for density, and  $\chi$  stands for volume fraction of each phase. Since the density of MgO is more than that of aluminum, it is anticipated that with increasing the MgO volume percent, density of composites increases which is evident in the values of theoretical densities. Theoretical densities of the nanocomposites are equal to 2.71, 2.72, and 2.74 g cm<sup>-3</sup> for MgO contents of 1.5, 2.5, 5 vol.%, respectively.

It can be seen that the density increases with the MgO content at 850 °C. This behavior is consistent with the mixture rule in which the total density increases with the volume percent of the second phase [35]. For the composites, cast at 800 and 950 °C, increasing the volume content of MgO led to an increase of the density up to 2.5 %. Then, density followed a decreasing trend which is due to the effect of high temperature (950 °C) and agglomeration at high content of reinforcement. Moreover, tensile stresses originated from thermal expansion coefficient

mismatch between metal matrix and rigid reinforcement (CTE of aluminum and MgO are  $21.50 \times 10^{-6}$  and  $14.45 \times 10^{-6} \text{ } ^\circ\text{C}^{-1}$ , respectively), would normally form defects such as porosity and dislocations around the particles [23, 36–38].

According to the above explanations, bulk densities of the nanocomposites have not a regular trend with increasing the MgO content, or the casting temperature and the incremental trend in theoretical density are not exactly followed by the bulk density. However, the values obtained for bulk densities of the nanocomposites are remarkably close to the corresponding theoretical density values and all of the samples achieved a  $[D_{\text{Bulk}}]/[D_{\text{Theoretical}}]$  ratio of more than 97.3 %. In other words, the porosity factor of none of the samples is higher than 2.70 %. Porosity factor is derived from the ratio of bulk density to theoretical density and is equal to subtraction of this ratio from 100. Porosity factor indicates an amount of undesirable pores and voids which are formed during the casting process (and also, could be intensified with increasing casting temperature and reinforcement content because of air entrapment due to high fluidity and viscosity of the melt at each variable, respectively), and is the main reason that causes diversity between bulk and theoretical densities. These kinds of interstices are different from contraction cavity and unlike that are tended to be distributed in the whole body of the sample in the shape of small and sometimes microscopic voids. Similar to the bulk density, the values of porosity factors have an arbitrary trend with increasing the MgO volume fraction or casting temperature. However, it could be expected that with increasing the content of ceramic phase the amount of porosity increases since a reasonable wettability becomes harder to achieve. In this sense, it is anticipated that samples cast at higher temperatures would achieve higher bulk density or less porosity, because it improves wettability. Such decreasing trend is somehow recognizable with increasing the casting temperature. Yet, the least amount of porosity is achieved at casting temperature of 850 °C (in 5 vol.% MgO). The other samples also have very similar percentage of porosity. Finally, it can be concluded that composite cast at 850 °C represents maximum compatibility and can be considered as the optimum fabrication condition. Also, according to porosity chart (Fig. 2b), it can be deduced that 2.5 vol.% MgO – for all temperatures – is the best amount of reinforcement phase.

### 3.2. XRD analysis

The phases identified by XRD analysis were similar for all composites. Although, their peak intensity was different but magnesium oxide (MgO), silicon (Si) and aluminum (Al) were just detected. Figure 3 shows the XRD pattern of nanocomposite containing 2.5 vol.%

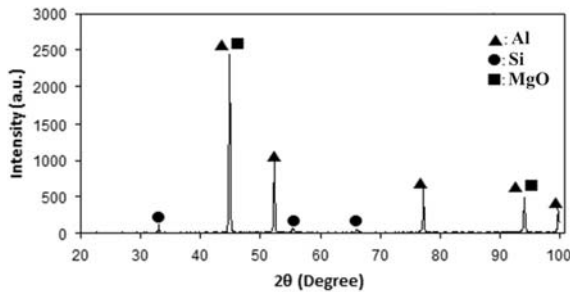


Fig. 3. XRD pattern of Al-2.5MgO nanocomposite cast at 850°C.

of MgO fabricated at 850°C. All peaks could be indexed as cubic (fcc) aluminum and MgO. No further crystallographic structure was detected in XRD pattern. This shows that no substantial interactions take place between the base metal and reinforcement phase during casting which may result in formation of intermetallic phases. The relatively intense peaks of MgO are a sign of almost uniform distribution of ceramic particles in metal matrix.

### 3.3. Microstructural studies

To better understand the effect of porosity on the characteristics of Al/MgO nanocomposites, the microstructures of the cast samples were studied via SEM. Scanning electron micrographs of the as-cast Al/MgO nanocomposites with different amount of reinforcement phase, cast at 800, 850, and 950°C, are presented in Figs. 4–8. The images are taken in BSE (back-scattered electron) mode in order to distinguish between different phases based on the difference of average atomic numbers of each phase, mainly A356.1 matrix, MgO, and pores. In this respect, the notable microstructural phenomena are agglomerations and porosity voids which appear as lighter and darker areas compared with ambient gray color of background, respectively. As mentioned in section 3.1., MgO has a higher density than aluminum alloy matrix, and so tends to appear brighter, accordingly. Notwithstanding, uniform distribution of reinforcement particles of MgO is attained in non-agglomerate areas (background area).

In all sets of images, it could be observed that with increasing the volume percent of MgO the scale of agglomeration and consequent microstructural deteriorations as porosity increase. The agglomerated regions appears as brighter MgO-rich particles in the rather darker background which chiefly consists of aluminum. The porosity of samples tends to grow and propagate with increasing the amount of MgO which confirms the results of density measurements. On the other hand, the microstructural quality of the nanocomposites is rather improved and the amount of agglomera-

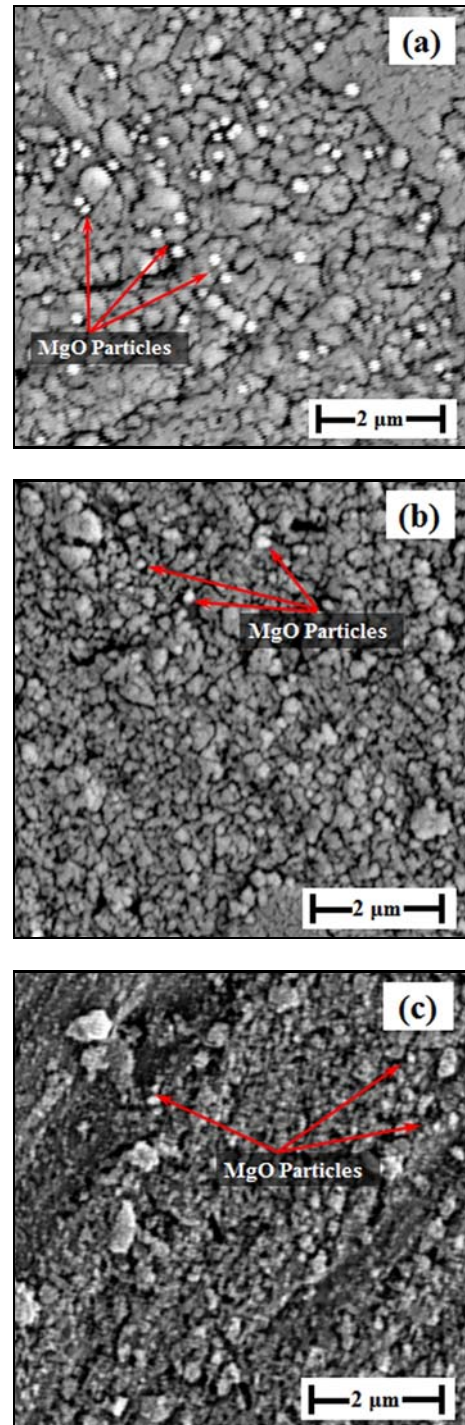


Fig. 4. Scanning electron micrographs of the Al/MgO nanocomposites with different amounts of reinforcement phase, cast at 800°C: 1.5 (a), 2.5 (b), 5 (c) vol.% MgO.

tion and porosity has diminished with increasing the casting temperature.

To better demonstrate the extent of the agglomeration in Al/MgO nanocomposites produced using stir casting method, a set of images showing the X-ray mapping of samples cast at 850°C with their corres-

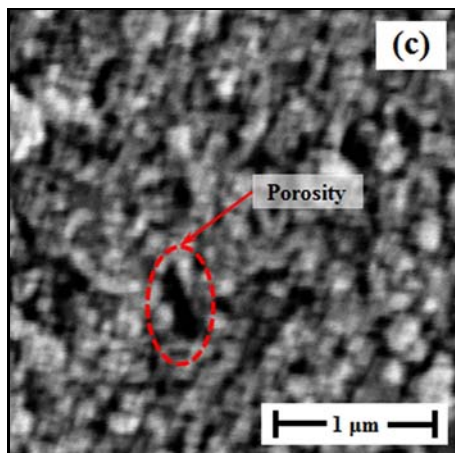
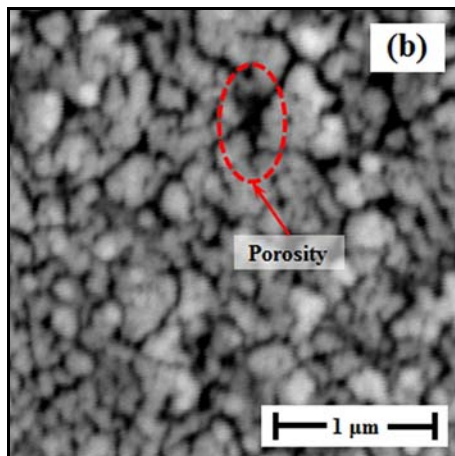
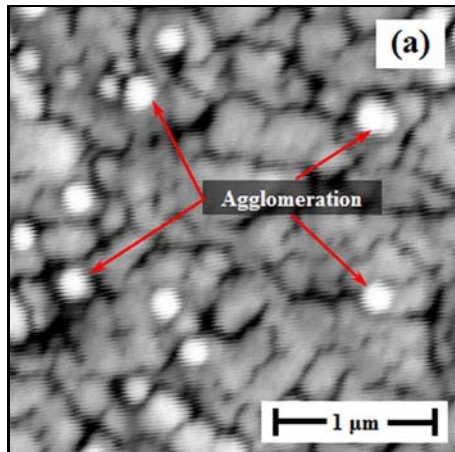


Fig. 5. Scanning electron micrographs of the Al/MgO nanocomposites with different amounts of reinforcement phase, cast at 800°C: 1.5 (a), 2.5 (b), 5(c) vol.% MgO at higher magnification.

ponding SEM images is presented in Fig. 7. As can be seen, those lump-like protrusions – seen also in other figures – are the areas with higher concentrations of magnesium and oxygen (related to MgO) that indicate the agglomeration of the ceramic phase. These areas occur as dense dots of Mg and O in the elemental

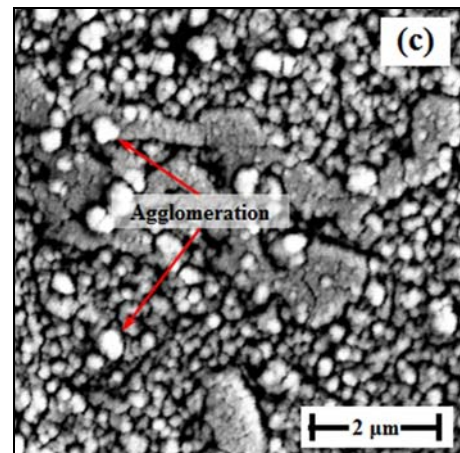
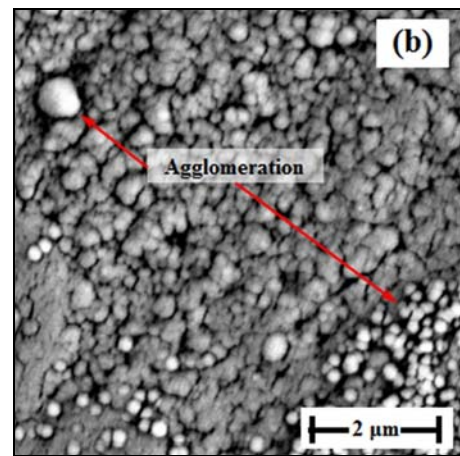
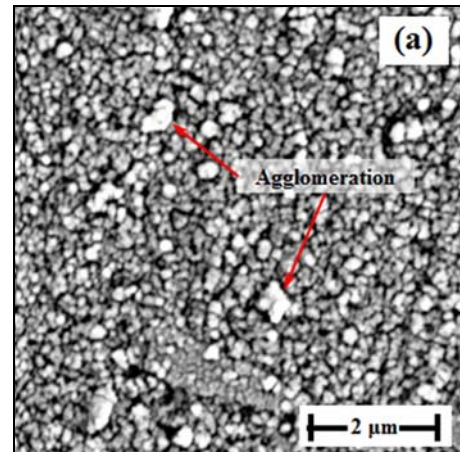


Fig. 6. Scanning electron micrographs of the Al/MgO nanocomposites with different amounts of reinforcement phase, cast at 850°C: 1.5 (a), 2.5 (b), 5 (c) vol.% MgO.

maps. In spite of regional agglomerations, a uniform distribution of reinforcement particles can clearly be observed in the map images, which is in agreement with XRD results and previous explanations of SEM images.

Several reasons are proposed to justify the quality

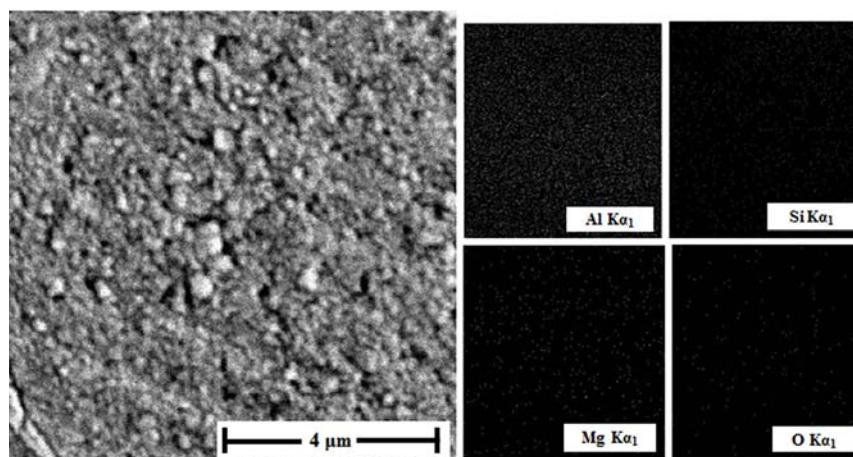


Fig. 7. X-ray mapping and the corresponding SEM images of the Al/MgO nanocomposites with different amounts of reinforcement phase cast at 850°C with 5 vol.% MgO.

of ceramic particles distribution and the occurrence of porosity and severe agglomeration in as-cast composites which generally involves the phenomena arisen during casting process and especially those that occur in the solidification area. The interface between solid and melt phases moves during solidification, known as solidification front. In this step, particles may be entrapped in the solid phase, pushed away by the surface of the solid phase, or in some rare cases, nucleation may occur on the surface of ceramic particles which are identified as pushing, entrapment, and engulfment mechanisms, respectively. Between these mechanisms, engulfment could be regarded as the ideal one, since it causes individual distribution of particles and avoids agglomeration. But, the main requisite for engulfment is proper wettability of particles with a matrix which is remarkably poor for most of ceramics and thus, engulfment is not the dominant mechanism [8, 27]. Moreover, heterogeneous nucleation takes place in the surface of the metallic mold since it is rapidly cooled during solidification. Therefore, a combination of entrapment and mainly pushing mechanisms is responsible for distribution of particles in the system. During solidification, alloying elements (mainly Si) and MgO particles are pushed away by liquid/solid interface [27]. Due to this phenomenon silicon embryos are transferred to the surface of MgO agglomerates and solidify at those places. Nucleation of Si on the surface of MgO particles can be explained regarding the bonding nature of silicon and MgO which is metalloid and ionic, respectively. Hence, these two components have substantially lower stress in their interface rather than Al/Si and Al/MgO interfaces. The supremacy of pushing mechanism is reduced with increasing the additive, while the superiority of entrapment mechanism is enhanced with increasing the MgO content. MgO particles would be entrapped between the dendrite arms with progress of the solidification front and increasing the MgO concentration in the li-

quid phase. Therefore, it is expected that the distribution of ceramic phase improves at the center of the composites [27, 28].

Casting temperature, solidification and mixing time, volume fraction of additives, and the size of the particles are the main parameters that govern homogeneity of particle distribution in the matrix. Nanometric size of the reinforcement particles could also cause growth and propagation of porosity due to higher surface area, higher surface tension, higher tendency to agglomerate, and increasing the viscosity of melt. Furthermore, the suction of air through the melt in vortex method could cause air entrapment and formation of gas pores. Increasing the casting temperature diminishes the amount of porosity due to improvement in wettability, but could also cause some undesirable destructive reactions between Al melt and reinforcement phase.

#### 4. Conclusions

Results presented in this investigation reveal the effect of the reinforcement content and the casting temperatures on the density and microstructure of Al-MgO nanocomposites which were fabricated by the stir casting method. Production of Al-MgO nanocomposites with MgO nanoparticles has been successfully accomplished using this method. Density measurements of fabricated samples revealed that the bulk density of samples increased with increasing the vol.% of MgO up to 2.5 %, for all three temperatures. But the density for cast samples at 800 and 950°C followed decreasing trend which was due to the negative effect of pores generation and agglomeration at high content of reinforcement. In fact, the incremental trend for the bulk density was dominant at 850°C. However, the values obtained for bulk densities of the nanocomposites (of all the samples) are remarkably

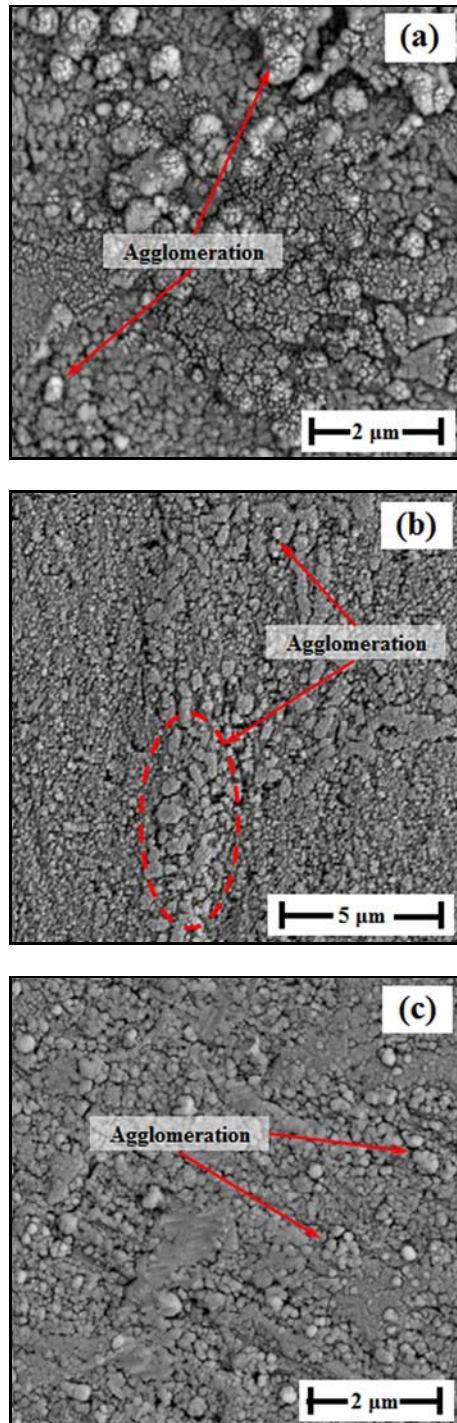


Fig. 8. Scanning electron micrographs of the Al/MgO nanocomposites with different amounts of reinforcement phase, cast at 950 °C: 1.5 (a), 2.5 (b), 5 (c) vol.% MgO.

close to the corresponding theoretical density values. XRD phase analysis approved the uniform presence of MgO in Al matrix with no signs of formation of other intermetallic phases. SEM micrographs of the samples illustrated a uniform distribution of reinforcement particles in the matrix alloy, in spite of regional

agglomerations. At last, among the other processing temperatures, 850 °C could be selected as the optimum temperature to achieve better properties.

## References

- [1] Hatch, J. E.: Aluminum: Properties and Physical Metallurgy. Metal Park, OH, ASM 1984.
- [2] Hull, D.: An Introduction to Composite Materials. New York, Cambridge University Press 1981.
- [3] Ekici, R., Apalak, M. K., Yildirim, M.: Composites Part B: Eng., 42, 2011, p. 1497. [doi:10.1016/j.compositesb.2011.04.053](https://doi.org/10.1016/j.compositesb.2011.04.053)
- [4] Qing, H.: Mater. Design, 51, 2013, p. 438. [doi:10.1016/j.matdes.2013.04.051](https://doi.org/10.1016/j.matdes.2013.04.051)
- [5] Barmouz, M., Besharati Givi, M. K., Seyfi, J.: Mater. Characterization, 62, 2011, p. 108. [doi:10.1016/j.matchar.2010.11.005](https://doi.org/10.1016/j.matchar.2010.11.005)
- [6] Kumar, A., Lal, S., Kumar, S.: Mater. Research Technol., 2, 2013, p. 250. [doi:10.1016/j.imrt.2013.03.015](https://doi.org/10.1016/j.imrt.2013.03.015)
- [7] Kim, E. H., Cho, G. H., Lee, J. H., Jung, Y. G., Yoo, Y. S., Seo, S. M.: J. Ceram. Inter., 39, 2013, p. 6503. [doi:10.1016/j.ceramint.2013.01.082](https://doi.org/10.1016/j.ceramint.2013.01.082)
- [8] Hashim, J., Looney, L., Hashmi, M. S. J.: Mater. Process. Technol., 92–93, 1999, p. 1. [doi:10.1016/S0924-0136\(99\)00118-1](https://doi.org/10.1016/S0924-0136(99)00118-1)
- [9] Skibo, D. M., Schuster, D. M., Jolla, L.: US Patent No. 4 786 467, 1988.
- [10] Reyes, M., Canul, M., Torres, J.: Ceram. Int., 37, 2011, p. 2719. [doi:10.1016/j.ceramint.2011.04.028](https://doi.org/10.1016/j.ceramint.2011.04.028)
- [11] Li, G., Zhao, Y., Wang, H., Chen, G., Dai, Q., Cheng, X.: Alloy Compd., 471, 2009, p. 530. [doi:10.1016/j.jallcom.2008.04.037](https://doi.org/10.1016/j.jallcom.2008.04.037)
- [12] Safari, J., Chermahini, M., Akbari, G.: Powder Technol., 234, 2013, p. 7. [doi:10.1016/j.powtec.2012.09.033](https://doi.org/10.1016/j.powtec.2012.09.033)
- [13] Wang, H., Jiang, Q., Wang, Y., Ma, B., Zhao, F.: Mater. Letter., 58, 2004, p. 3509. [doi:10.1016/j.matlet.2004.04.038](https://doi.org/10.1016/j.matlet.2004.04.038)
- [14] Abdizadeh, H., Baghchesara, M. A.: J. Mech. Sci. Technol., 26, 2012, p. 367. [doi:10.1007/s12206-011-1101-9](https://doi.org/10.1007/s12206-011-1101-9)
- [15] Qu, H., Zhu, S., Li, Q.: Ceram. Int., 38, 2012, p. 1371. [doi:10.1016/j.ceramint.2011.09.016](https://doi.org/10.1016/j.ceramint.2011.09.016)
- [16] Naher, S., Brabazon, D., Looney, L.: Mater. Process. Tech., 166, 2004, p. 430. [doi:10.1016/j.jmatprotec.2004.09.043](https://doi.org/10.1016/j.jmatprotec.2004.09.043)
- [17] Rohatgi, P. K.: Key Eng. Mater., 104–107, 1995, p. 283. [doi:10.4028/www.scientific.net/KEM.104-107.283](https://doi.org/10.4028/www.scientific.net/KEM.104-107.283)
- [18] Degischer, H. P.: Mater Design, 18, 1997, p. 221. [doi:10.1016/S0261-3069\(97\)00054-X](https://doi.org/10.1016/S0261-3069(97)00054-X)
- [19] Su, H., Gao, W., Feng, Z., Lu, Z.: Mater. Design, 36, 2012, p. 590. [doi:10.1016/j.matdes.2011.11.064](https://doi.org/10.1016/j.matdes.2011.11.064)
- [20] Lai, J., Zhang, Z., Chen, X. G.: Alloy Compd., 552, 2013, p. 227. [doi:10.1016/j.jallcom.2012.10.096](https://doi.org/10.1016/j.jallcom.2012.10.096)
- [21] Zhang, Q., Ma, X., Wu, G.: Ceram. Int., 39, 2013, p. 4893. [doi:10.1016/j.ceramint.2012.11.082](https://doi.org/10.1016/j.ceramint.2012.11.082)
- [22] Chen, Y., Abraham, M. M., Robinson, M. T.: In: Proceedings of Intern. Conf. on Radiation Effects and Tritium Tech Fusion Reactors- MAGNESIUM OXIDE (MgO) – Advanced Energy Technology Program.

- Eds.: Watson, J. S., Wiffen, F. W. Gatlinburg, Tennessee, USA, National Technical Information Service (ntis.gov publisher) – CONF-750989-P3 1975, p. 492.
- [23] Abdizadeh, H., Ebrahimifard, R., Baghchesara, M. A.: *Composites Part B: Eng.*, *56*, 2014, p. 217. [doi:10.1016/j.compositesb.2013.08.023](https://doi.org/10.1016/j.compositesb.2013.08.023)
- [24] Mizuuchi, K., Inoue, K., Agari, Y., Sugioka, M., Tanaka, M., Takeuchi, T., Kawahara, M., Makino, Y., Ito, M.: *Composites Part B: Eng.*, *43*, 2012, p. 1445. [doi:10.1016/j.compositesb.2011.08.003](https://doi.org/10.1016/j.compositesb.2011.08.003)
- [25] Mandal, D., Viswanathan, S.: *Materials Characterization*, *86*, 2013, p. 21. [doi:10.1016/j.matchar.2013.09.008](https://doi.org/10.1016/j.matchar.2013.09.008)
- [26] Mizuuchi, K., Inoue, K., Agari, Y., Sugioka, M., Tanaka, M., Takeuchi, T., Kawahara, M., Makino, Y., Ito, M.: *Composites Part B: Eng.*, *42*, 2011, p. 1029. [doi:10.1016/j.compositesb.2011.03.028](https://doi.org/10.1016/j.compositesb.2011.03.028)
- [27] Daoud, A., Abo-Elkhar, M.: *Mater. Process. Technol.*, *120*, 2002, p. 296. [doi:10.1016/S0924-0136\(01\)01067-6](https://doi.org/10.1016/S0924-0136(01)01067-6)
- [28] Karnezis, P. A., Durrant, G., Canter, B.: *Mater. Sci. Technol.*, *11*, 1995, p. 741. [doi:10.1179/mst.1995.11.8.741](https://doi.org/10.1179/mst.1995.11.8.741)
- [29] Davies, C. H. J.: *Key Eng. Mater.*, *104–107*, 1995, p. 447. [doi:10.4028/www.scientific.net/KEM.104-107.447](https://doi.org/10.4028/www.scientific.net/KEM.104-107.447)
- [30] Stefanescu, D. M., Dhindaw, B. K., Kacar, S. A., Mottra, A.: *Metall. Trans. A*, *19*, 1998, p. 2847. [doi:10.1007/BF02645819](https://doi.org/10.1007/BF02645819)
- [31] Gagnon, G., Chawla, K., Rezai, F., Ilschner, B.: *Zeitschrift für Metallkunde*, *85*, 1994, p. 312.
- [32] Stefanescu, D. M., Moitra, A., Kacar, A., Dhindaw, B. K.: *Metall. Trans. A*, *21*, 1990, p. 231. [doi:10.1007/BF02656440](https://doi.org/10.1007/BF02656440)
- [33] Sasikumar, R., Kumar, M.: *Acta Materialia*, *39*, 1991, p. 2503. [doi:10.1016/0956-7151\(91\)90065-9](https://doi.org/10.1016/0956-7151(91)90065-9)
- [34] Dutta, B., Surappa, M. K.: *Metall. Trans. A*, *29*, 1998, p. 1329. [doi:10.1007/s11661-998-0259-y](https://doi.org/10.1007/s11661-998-0259-y)
- [35] Spowart, J. E., Maruyama, B., Miracle, D. B.: *Mater. Sci. Eng. A*, *307*, 2001, p. 51. [doi:10.1016/S0921-5093\(00\)01962-6](https://doi.org/10.1016/S0921-5093(00)01962-6)
- [36] Abdizadeh, H., Baghchesara, M. A.: *Ceram. Int.*, *39*, 2012, p. 2045. [doi:10.1016/j.ceramint.2012.08.057](https://doi.org/10.1016/j.ceramint.2012.08.057)
- [37] Almeida, M., Brook, R., Carruthers, T.: *Mater. Sci.*, *14*, 1979, p. 2191. [doi:10.1007/BF00688425](https://doi.org/10.1007/BF00688425)
- [38] Khorrarnie, S. A., Baghchesara, M. A., Gohari, D. P.: *Trans. Nonferrous Met. Soc. China*, *23*, 2013, p. 1556. [doi:10.1016/S1003-6326\(13\)62630-8](https://doi.org/10.1016/S1003-6326(13)62630-8)